Spectroscopy and decay properties of charmonium

Virendrasinh Kher[1,2;1)] Ajay Kumar Rai[2;2)]

[1] Applied Physics Department, Polytechnic, The M.S. University of Baroda, Vadodara 390002, Gujarat, India
[2] Department of Applied Physics, Sardar Vallabhbhai National Institute of Technology, Surat 395007, Gujarat, India

Abstract: The mass spectra of charmonium are investigated using a Coulomb plus linear (Cornell) potential. Gaussian wave functions in position space as well as in momentum space are employed to calculate the expectation values of potential and kinetic energy respectively. Various experimental states ($X(4660)(5^3S_1)$, $X(3872)(2^3P_1)$, $X(3900)(2^1P_1)$, $X(3915)(2^3P_0)$ and $X(4274)(3^3P_1)$ etc.) are assigned as charmonium states. We also study the Regge trajectories, pseudoscalar and vector decay constants, electric and magnetic dipole transition rates, and annihilation decay widths for charmonium states.

Keywords: potential model, mass spectrum, decay constant, Regge trajectories

PACS: 12.39.Jh, 12.40.Yx, 13.20.Gd **DOI:** 10.1088/1674-1137/42/8/083101

1 Introduction

The discovery of the J/ψ, the first bound state of c and $\overline{c}$ quarks, known as charmonium, was published in Ref. [1]. Reference [2] describes the first observation of the ψ(2S), marking the field of hadron spectroscopy with the beginning of an important testing ground for the properties of the strong interaction using QCD. The charmonium system allows the prediction of some of the parameters of the states using non-relativistic and relativistic potential models, lattice QCD, NRQCD and sum rules [3]. Although the first charmonium state was discovered in 1974, there are still many puzzles in charmonium physics. Charmonium spectroscopy below the open charm threshold has been well measured and agrees with the theoretical expectations. However, there is still a lack of adequate experimental information and solid theoretical predictions for the charmonium states above the open charm threshold [4]. Recently many other new resonances, named the XYZ particles, have been discovered and are still under examination, as these states do not match the predictions of the non-relativistic or semi-relativistic $q\bar{q}$ potential models.

In 1976, Siegrist and others in the MARK-I Collaboration (SLAC) observed the resonance ψ(4415) with mass 4415 ± 7 MeV [5]. In 1978, the DASP Collaboration observed peaks for the ψ(4040), ψ(4160) and ψ(4415) resonances with masses 4040±10, 4159±20 and 4417 ± 10 MeV respectively using a non-magnetic detector [6]. Ablikim and others in the BES Collaboration and Mo and others at the Institute of High Energy Physics, Beijing, determined the resonance parameters for ψ(4040), ψ(4160) and ψ(4415) charmonium. Eichten identified these three resonances as 3^3S_1, 2^3D_1 and 4^3S_1 with a linear plus Coulomb potential model [7], and most later potential model calculations agree with their identification. Recently, the LHCb Collaboration measured the mass 4191^{+9}_{-8} MeV of the resonance ψ(4160) with $J^{PC} = 1^{--}$ [8]. In 2007, a resonant structure was observed by the Belle Collaboration with mass 4664±11±5 MeV [9]. A year later the same collaboration observed a clear peak in the $e^+e^- \to \Lambda_c^+\Lambda_c^-$ invariant mass distribution and assumed the observed peak to be a resonance of mass 4634^{+8+5}_{-7-8} MeV with the possibility of a 5^3S_1 charmonium state [10].

Rapidis and others at SLAC, the LGW Collaboration, observed a resonance with mass 3772±6 MeV, just above the threshold for the production of charmed particles [11]. In a parallel observation, W. Bacino and others at SLAC discovered and confirmed the ψ(3770) resonance with mass 3770±6 MeV [12] and the parameters were determined by the SLAC and LBL Collaborations [13]. In 2006 the BES Collaboration measured the mass of the ψ(3770) resonance precisely [14], and recently its parameters have been measured using the data collected with the KEDR detector [15]. The Belle Collaboration reported the first observation of a new charmonium-like state with mass $3943 \pm 6 \pm 6$ MeV in the spectrum of

Received 29 March 2018, Published online 20 June 2018

1) E-mail: vhkher@gmail.com
2) E-mail: raiajayk@gmail.com

masses recoiling from the J/ψ in the inclusive process $e^+e^- \to J/\psi$+anything, and denoted it as $X(3940)$ [16]. Later on, a new measurement for the $X(3940)$ was performed by the same collaboration and the mass $3942^{+7}_{-6}\pm6$ MeV was reported [17]. The 3^1S_0 state is a good candidate for the $X(3940)$ resonance [18, 19].

Evidence of a new narrow resonance $X(3823)$ was found by Belle [20], with its mass near to potential model expectations for the centroid of the 1^3D_J states. Recently, the BESIII Collaboration [21] observed a narrow resonance $X(3823)$ through the process $e^+e^- \to \pi^+\pi^-X(3823)$ and confirmed that it is a good candidate for the $\psi(1^3D_2)$ charmonium state.

In 2003, the Belle Collaboration observed a charmonium-like state in the decay process $B^\pm \to K^\pm\pi^+\pi^-J/\psi$ with mass $3872\pm0.6\pm0.5$ MeV [22], which was confirmed by the CDF, D0 and BaBar experiments [23–25]. Several properties of the $X(3872)$ have been determined [26–28], and the CDF Collaboration explained the X(3872) particle as a conventional charmonium $c\bar{c}$ state with J^{PC} being either 1^{++} or 2^{-+} [29]. Recently the BESIII Collaboration reported the first observation of process $e^-e^- \to \gamma X(3872)$ with mass $3871\pm0.7\pm0.2$ MeV [30]. In 2003, Barnes and Godfrey evaluated the strong and electromagnetic decays and considered all possible 1D and 2P charmonium assignments for $X(3872)$ [31].

The $X(3915)$ was observed by S.K. Choi and his team at the Belle Collaboration [32] and later on the BaBar Collaboration confirmed the existence of the charmonium-like resonance $X(3915)$ and measured its mass $3919.4\pm2.2\pm1.6$ MeV with the $J^{PC}=0^{++}$ option [33, 34]. This state is conventionally identified as the $\chi_{c0}(2P)$ charmonium [35, 36]. In 2005, the Belle Collaboration observed the $Z(3930)$ resonance in the $\gamma\gamma \to D\bar{D}$ process [37] with mass $3929\pm5\pm2$ MeV and considered it a strong candidate for the $\chi_{c2}(2P)$ state. The BaBar Collaboration confirmed the $Z(3930)$ resonance as the $\chi_{c2}(2P)$ state with mass $3926.7\pm2.7\pm1.1$ MeV and quantum numbers $J^{PC}=2^{++}$ [38].

In 2013, the BESIII Collaboration observed a new structure with mass $3899\pm3.6\pm4.9$ MeV in the $\pi^\pm J/\psi$ mass spectrum (referred as $Z_c(3900)$) [39] and around the same time the Belle Collaboration observed a structure with mass $3894.5\pm6.6\pm4.5$ MeV in the $\pi^\pm J/\psi$ mass spectrum [40]. The observations of Xiao and his team, based on e^+e^- annihilations at $\sqrt{s}=4170$ MeV, provide independent confirmation of the existence of the $Z_c^\pm(3900)$ state and provide new evidence for the existence of the neutral state $Z_c^0(3900)$ [41]. Recently the BESIII Collaboration performed an analysis which favors the assignment of the $J^P=1^+$ quantum numbers [42].

In 2009, the CDF Collaboration reported evidence for a narrow structure near the $J/\psi\phi$ threshold in $B^+ \to J/\psi\phi K^+$ decays with mass $4143\pm2.9\pm1.2$ MeV [43], which was recently observed by the CMS [44] and D0 [45, 46] Collaborations. It has been suggested that the $X(4140)$ resonance could be a molecular state [47–50], a tetra-quark state [51–53] or a hybrid state [54, 55]. Searches for the narrow $X(4140)$ were negative in the LHCb [56] and BaBar [57] experiments. In 2011, the CDF Collaboration observed the $X(4140)$ structure with a statistical significance greater than 5 standard deviations and also found evidence for a second structure $X(4274)$ with a mass of $4274.4^{+8.4}_{-6.7}\pm1.9$ MeV [58]. Very recently the LHCb Collaboration confirmed the resonance $X(4140)$ with mass $4146.5\pm4.5^{+4.6}_{-2.8}$ MeV and $X(4274)$ with mass $4273.3\pm8^{+17.2}_{-3.6}$ MeV in the $J/\psi\phi$ invariant mass distribution, and determined their spin-parity quantum numbers to be $J^{PC}=1^{++}$ for both [59]. They also investigated two new structures, named the $X(4500)$ and $X(4700)$, in the high $J/\psi\phi$ mass region. Reference [60] suggests that $X(4274)$ can be a good candidate for the conventional $\chi_{c1}(3^3P_1)$ state. The study of charmonium in the relativistic Dirac formalism with a linear confinement potential indicates that the $X(4140)$ state can be an admixture of two P states whereas $X(4630)$ and $X(4660)$ are admixtures of the S-D wave state [61].

Different theoretical models which have been used to study the charmonium spectrum include the recently developed generalized screened potential model (GSPM) [62], the non-relativistic Coulomb gauge QCD approach [63], the light front quark model (LFQM) [64], the relativistic quark model [65], the effective field theory framework of potential non-relativistic QCD (pNRQCD) approach [66], the effective Lagrangian approach [67], lattice QCD [68, 69], LCQCD and QCD sum rules [70, 71], and the widely used potential models [72–78]. The Cornell potential model is well known among the many phenomenologically successful potential models, and describes the charmonium system quite well.

The recent experimental results for the new charmonium-like XYZ states indicate that they can be interpreted as above-threshold charmonium levels and cannot be assigned to any charmonium states in the conventional quark model. These experimental results motivate renewed theoretical interest in studies of the spectroscopy and decay properties of charmonium.

In this article, to calculate the mass spectrum of charmonium, we use Gaussian wave functions both in position space as well as momentum space with a potential model, incorporating corrections to the kinetic energy of quarks as well as incorporating the relativistic correction of $\mathcal{O}\left(\frac{1}{m}\right)$ to the potential energy part of the Hamiltonian. We also investigate the Regge trajectories in both the $(M^2 \to J)$ and $(M^2 \to n)$ planes (where J is the spin and n is the principal quantum number) using our

predicted masses for the charmonium, as the Regge trajectories play a significant role in identifying the nature of current and future experimentally observed charmonium states. We also obtain the pseudoscalar and vector decay constants for charmonium as well as the radiative (electric and magnetic dipole) transition rates and the annihilation decay.

The article is organized as follows. Section 2.1 presents the theoretical framework for the mass spectra, Section 2.2 presents the decay constants ($f_{P/V}$), Section 2.3 presents the radiative (E1 and M1) transitions, and Section 2.4 presents the annihilation decays. In Section 3, we discuss results for the mass spectra, ($f_{P/V}$) decays, E1 and M1 transition width, and annihilation decays. The Regge trajectories from estimated masses in the (J,M^2) and (n_r,M^2) planes are given in Section 3.1. Finally, we draw our conclusion in Section 4.

2 Method

2.1 Cornell potential with $\mathcal{O}\left(\frac{1}{m}\right)$ corrections

Here we calculate the mass spectra and decay properties of charmonium within the widely used Coulomb plus linear potential, the Cornell potential [72, 73, 79, 80]. In this approach, we consider the relative corrections to the kinetic energy part and $\mathcal{O}\left(\frac{1}{m}\right)$ correction to the potential energy part [81–84], which is inspired from the pNRQCD (potential non-relativistic quantum chromodynamics) [3, 85, 86]. The Cornell potential works well for heavy light flavour, hence we employed it for heavy-heavy flavour.

We employ the following Hamiltonian [82–84, 87, 88] and quark-antiquark potential [81] to study the charmonium mass spectroscopy,

$$H=\sqrt{\boldsymbol{p}^2+m_Q^2}+\sqrt{\boldsymbol{p}^2+m_{\bar{Q}}^2}+V(\boldsymbol{r}), \tag{1}$$

$$V(r)=V^{(0)}(r)+\left(\frac{1}{m_Q}+\frac{1}{m_{\bar{Q}}}\right)V^{(1)}(r)+\mathcal{O}\left(\frac{1}{m^2}\right). \tag{2}$$

Here, $m_Q(m_{\bar{Q}})$ is the quark(anti-quark) mass. The Cornell-like potential $V^{(0)}$ [78] and $V^{(1)}(r)$ from leading order perturbation theory are,

$$V^{(0)}(r)=-\frac{4\alpha_S(M^2)}{3r}+Ar+V_0, \tag{3}$$

$$V^{(1)}(r)=-C_FC_A\alpha_s^2/4r^2, \tag{4}$$

where $\alpha_S(M^2)$ is the strong running coupling constant, A is the potential parameter, V_0 is the potential constant, and $C_F=4/3$, $C_A=3$ are the Casimir charges. This correction was originally studied by Y. Koma, where the relativistic correction to the QCD static potential $\mathcal{O}\left(\frac{1}{m}\right)$ was investigated non-perturbatively. This correction was found to be similar to the Coulombic term of the static potential when applied to charmonium. The leading order corrections are classified in powers of the inverse of heavy quark mass [81].

Here, to estimate the expected values of the Hamiltonian with the Ritz variational strategy, we use a Gaussian wave function in position space as well as in momentum space [83, 84] which has the form

$$R_{nl}(\mu,r) = \mu^{3/2}\left(\frac{2(n-1)!}{\Gamma(n+l+1/2)}\right)^{1/2}(\mu r)^l \times e^{-\mu^2r^2/2}L_{n-1}^{l+1/2}(\mu^2r^2), \tag{5}$$

and

$$R_{nl}(\mu,p) = \frac{(-1)^n}{\mu^{3/2}}\left(\frac{2(n-1)!}{\Gamma(n+l+1/2)}\right)^{1/2}\left(\frac{p}{\mu}\right)^l \times e^{-p^2/2\mu^2}L_{n-1}^{l+1/2}\left(\frac{p^2}{\mu^2}\right), \tag{6}$$

respectively with the Laguerre polynomial L and the variational parameter μ. We estimated μ for each state, for the preferred value of A, using [88],

$$\langle K.E.\rangle=\frac{1}{2}\left\langle\frac{r\mathrm{d}V}{\mathrm{d}r}\right\rangle. \tag{7}$$

To integrate the relativistic correction, we enlarge the Hamiltonian (1) with powers up to $\mathcal{O}(\boldsymbol{p}^{10})$ and $\mathcal{O}\left(\frac{1}{m}\right)$ for the kinetic energy and the potential energy part respectively [83]. We use a position space Gaussian wave function to obtain the expected value of the potential energy part, whereas for the kinetic energy part, we use a momentum space wave function using virial theorem (Eq. (7)).

We adapted the ground state center of weight mass and equated with the PDG data by fixing A, α_s and V_0 using the following equation [89, 90]:

$$M_{SA}=M_P+\frac{3}{4}(M_V-M_P). \tag{8}$$

We also forecast the center of weight mass for the nJ state as [89]:

$$M_{CW,n}=\frac{\Sigma_J(2J+1)M_{nJ}}{\Sigma_J(2J+1)}. \tag{9}$$

In the case of quarkonia, bound states are represented by $n^{2S+1}L_J$, identified with the J^{PC} values, with $\vec{J}=\vec{L}+\vec{S}$, $\vec{S}=\vec{S}_Q+\vec{S}_{\bar{Q}}$, parity $P=(-1)^{L+1}$ and the charge conjugation $C=(-1)^{L+S}$ with (n,L) being the radial quantum numbers. The spin-dependent interactions are required to remove the degeneracy of charmonium states and can be written as [73, 91–93].

$$V_{SD} = V_{LS}(r)\left(\vec{L}\cdot\vec{S}\right)+V_{SS}(r)\left[S(S+1)-\frac{3}{2}\right] +V_T(r)\left[S(S+1)-\frac{3\left(\vec{S}\cdot\vec{r}\right)\left(\vec{S}\cdot\vec{r}\right)}{r^2}\right], \tag{10}$$

where the spin-spin, spin-orbit and tensor interactions can be written in terms of the vector and scalar parts of $V(r)$ as [92]

$$V_{SS}(r) = \frac{1}{3m_Q^2}\nabla^2 V_V = \frac{16\pi\alpha_s}{9m_Q^2}\delta^3(\vec{r}), \tag{11}$$

$$V_{LS}(r) = \frac{1}{2m_Q^2 r}\left(3\frac{\mathrm{d}V_V}{\mathrm{d}r} - \frac{\mathrm{d}V_S}{\mathrm{d}r}\right), \tag{12}$$

$$V_T(r) = \frac{1}{6m_Q^2}\left(3\frac{\mathrm{d}^2V_V}{\mathrm{d}r^2} - \frac{1}{r}\frac{\mathrm{d}V_V}{\mathrm{d}r}\right), \tag{13}$$

where $V_V(=-\frac{4\alpha_s}{3r})$ is the Coulomb part and $V_S(=Ar)$ is the confining part of Eq. (3)

In the present study, the quark masses is $m_c = 1.55$ GeV to reproduce the ground state masses of the charmonium. The fitted potential parameters are A=0.160 GeV^2, α_s=0.333 and V_0=−0.23074 GeV.

2.2 Decay constants ($f_{P/V}$)

The decay constants with the QCD correction factor are computed using the Van-Royen-Weisskopf formula [94, 95],

$$f^2_{P/V} = \frac{12|\psi_{P/V}(0)|^2}{M_{P/V}}\left(1-\frac{\alpha_S}{\pi}\left[2-\frac{m_Q-m_{\bar{q}}}{m_Q+m_{\bar{q}}}\ln\frac{m_Q}{m_{\bar{q}}}\right]\right). \tag{14}$$

Equation(14) also gives the inequality [96]

$$\sqrt{m_v}f_v \geqslant \sqrt{m_p}f_p. \tag{15}$$

Our results are in accordance with Eq. (15) and tabulated in Table 1. The value in parenthesis is the decay constant with QCD correction.

2.3 Radiative Transitions

The radiative transition is influenced by the matrix element of the EM current between the initial i and final f quarkonium state, i.e., $\langle f\,|\,j^{\mu}_{em}\,|\,i\rangle$. The electric dipole (E1) and magnetic dipole (M1) transitions are leading order transition amplitudes [97–99].

The E1 matrix elements are estimated by [100]

$$\Gamma_{(E1)}\left(n^{2S+1}L_J \to n'^{2S'+1}L'_{J'}+\gamma\right) = \frac{4\alpha e_Q^2}{3}\frac{E_\gamma^3 E_f}{M_i}C_{fi}\delta_{SS'}\times|\langle f|r|i\rangle|^2, \tag{16}$$

where photon energy $E_\gamma = \frac{M_i^2-M_f^2}{2M_i}$, the fine structure constant $\alpha = 1/137$, the quark charge is e_Q in units of electron charge, and the energy of the final state is E_f. The angular momentum matrix element C_{fi} is

$$C_{fi} = \max\left(L,L'\right)\left(2J'+1\right)\left\{\begin{array}{ccc} L' & J' & S \\ J & L & 1\end{array}\right\}^2, \tag{17}$$

where $\{:::\}$ is a 6-j symbol. The matrix elements $\langle n'^{2S'+1}L'_{J'}\,|\,r\,|\,n^{2S+1}L_J\rangle$ are evaluated using the wavefunctions

$$\langle f|r|i\rangle = \int \mathrm{d}r R_{n_i l_i}(r) R_{n_f l_f}(R). \tag{18}$$

The M1 radiative transitions are evaluated using the following expression [73, 101],

$$\Gamma_{M1}\left(n^{2S+1}L_J \to n'^{2S'+1}L'_{J'}\right) = \frac{4\alpha e_Q^2}{3m_Q^2}\frac{E_\gamma^3 E_f}{M_i}S_{fi}|\mathcal{M}_{fi}|^2, \tag{19}$$

where,

$$\mathcal{M}_{fi} = \int \mathrm{d}r R_{n_i l_i}(r) j_0(E_\gamma r/2) R_{n_f l_f}(R), \tag{20}$$

and

$$S_{fi} = 6(2S+1)\left(2S'+1\right)\left(2J'+1\right) \times\left\{\begin{array}{ccc} J & 1 & J' \\ S' & L & S\end{array}\right\}^2\left\{\begin{array}{ccc} 1 & 1/2 & 1/2 \\ 1/2 & S' & S\end{array}\right\}^2. \tag{21}$$

Here $L = 0$ for S-waves and $j_0(x)$ is the spherical Bessel function.

The E1 and M1 radiative transition widths are listed in Tables 5 and 6 respectively.

2.4 Annihilation decays

Decays of quarkonia states into leptons or photons or gluons are extremely useful for the production and identification of resonances as well as the leptonic decay rates of quarkonia. They can also assist to recognize conventional mesons and multi-quark structures [102, 103].

2.4.1 Leptonic decays

The $^3S_1$ and $^3D_1$ states have $J^{PC} = 1^{--}$ quantum numbers, and annihilate into lepton pairs through a single virtual photon. The leptonic decay width of the ($^3S_1$) and ($^3D_1$) states of charmonium, including first order radiative QCD correction, is given by [101, 102, 104]:

$$\Gamma(n^3S_1 \to e^+e^-) = \frac{4e_Q^4\alpha^2|R_{nS}(0)|^2}{M_{nS}^2}\left(1-\frac{16\alpha_s}{3\pi}\right), \tag{22}$$

$$\Gamma(n^3D_1 \to e^+e^-) = \frac{25e_Q^2\alpha^2|R''_{nD}(0)|^2}{2m_Q^4M_{nD}^2}\left(1-\frac{16\alpha_s}{3\pi}\right), \tag{23}$$

where M_{nS} is the mass of the decaying charmonium state.

2.4.2 Decay into photons

The annihilation decay of the charmonium states into two or three photons, without and/or with radiative QCD corrections are given by [101, 102]:

$$\Gamma(n^1S_0 \to \gamma\gamma) = \frac{3e_Q^4\alpha^2|R_{nS}(0)|^2}{m_Q^2}\left(1-\frac{3.4\alpha_s}{\pi}\right), \tag{24}$$

Table 1. Pseudoscalar and vector decay constants (in GeV).

decay	state	our work	Expt. [4]	Ref. [106]	Ref. [107]	Ref. [61]
f_P	1S	0.501(0.395)	0.335±0.075	0.471(0.360)	0.404	
	2S	0.301(0.237)		0.344(0.286)	0.331	
	3S	0.264(0.208)		0.332(0.254)	0.291	
	4S	0.245(0.193)		0.312(0.239)		
	5S	0.233(0.184)				
	6S	0.224(0.177)				
f_V	1S	0.510(0.402)	0.411±0.005	0.462(0.317)	0.375	0.420
	2S	0.303(0.239)	0.271±0.008	0.369(0.253)	0.295	0.285
	3S	0.265(0.209)	0.174±0.018	0.329(0.226)	0.261	0.218
	4S	0.240(0.194)		0.310(0.212)	0.240	0.166
	5S	0.234(0.185)		0.290(0.199)		0.106
	6S	0.225(0.177)				

Table 2. S-P-D-wave center of weight masses (in GeV). (LP = linear potential model, SP = screened potential model, NR = non-relativistic and RE = relativistic).

	this work		M_{SA} for other theories/GeV										
nL	μ /GeV	M_{SA} /GeV	Expt. [4] /GeV	LP (SP) [79]	Ref. [108]	Ref. [109]	Ref. [76]	NR (GI) [73]	Ref. [75]	Ref. [110]	Ref. [111]	RE(NR) [112]	Ref. [113]
$1S$	0.716	3.068	3.068	3.068(3.069)	3.090	3.067	3.061	3.063(3.067)	3.068	3.068	3.068	3.068(3.063)	3.068
$2S$	0.469	3.638	3.674	3.668(3.668)	3.667	3.673	3.676	3.662(3.663)	3.661	3.664	3.662	3.657(3.661)	3.665
$3S$	0.412	4.027		4.071(4.024)	4.070	4.027	4.080	4.065(4.091)	4.014	4.075	4.064	4.051(4.064)	4.090
$4S$	0.382	4.353		4.406(4.277)	4.408	4.421	4.406	4.400(4.444)	4.267			4.350(4.400)	
$5S$	0.363	4.646		4.706(4.469)	4.710	4.831			4.459			4.655(4.694)	
$6S$	0.349	4.917			4.987	5.164			4.603			4.907(4.973)	
$1P$	0.484	3.534	3.525	3.524(3.527)	3.523	3.525	3.525	3.522(3.523)	3.524	3.526	3.526	3.554(3.519)	3.523
$2P$	0.416	3.936		3.945(3.919)	3.941	3.926	3.945	3.942(3.961)	3.913	3.960	3.945	3.963(3.938)	3.962
$3P$	0.384	4.269		4.291(4.238)	4.289	4.337	4.316	4.286(4.323)	4.188			4.296(4.283)	
$1D$	0.437	3.802		3.805(3.805)	3.798	3.803	3.815	3.800(3.849)	3.796	3.823	3.811	3.839(3.799)	3.837
$2D$	0.396	4.150		4.164(4.108)	4.160	4.196	4.165	4.159(4.209)	4.099	4.190		4.187(4.158)	4.210
$3D$	0.372	4.455		4.478(4.336)	4.478	4.455	4.522		4.327			4.486(4.473)	

Table 3. Hyperfine and fine splittings (in MeV). (LP = linear potential model, SP = screened potential model, NR = non-relativistic and RE = relativistic).

splitting	this work	expt. [4]	other works									
			Ref. [79] LP(SP)	Ref. [108]	Ref. [109]	Ref. [73] NR(GI)	Ref. [76]	Ref. [75]	Ref. [110]	Ref. [112] RE (NR)	Ref. [111]	Ref. [61]
$m(1^3S_1)$-$m(1^1S_0)$	99	113.3±0.7	114 (113)	116	115	108 (123)	100	118	117	102 (108)	117	119
$m(2^3S_1)$-$m(2^1S_0)$	43	46.7±1.3	44 (42)	11	51	42 (53)	38	50	89	33 (42)	98	54
$m(3^3S_1)$-$m(3^1S_0)$	36		30 (26)	9	50	29 (36)	29	31	81	30 (29)	97	32
$m(4^3S_1)$-$m(4^1S_0)$	34		24 (17)	6	26	22 (25)	20	23		24 (22)		4.3
$m(5^3S_1)$-$m(5^1S_0)$	32		21 (13)	6	26			17		22 (19)		2.3
$m(6^3S_1)$-$m(6^1S_0)$	32			5	12			10		19 (17)		
$m(1^3P_2)$-$m(1^3P_1)$	33	45.5±0.2	36 (32)	47	44	51 (40)	41	44	50	41 (44)	46	
$m(1^3P_1)$-$m(1^3P_0)$	66	95.9±0.4	101 (106)	63	102	81 (65)	52	77	92	71 (80)	86	
$m(2^3P_2)$-$m(2^3P_1)$	31		30 (23)	46	45	47 (26)	38	36	54	40 (40)	43	
$m(2^3P_1)$-$m(2^3P_0)$	59		68 (66)	59	36	73 (37)	92	59	96	66 (73)	75	
$m(3^3P_2)$-$m(3^3P_1)$	33		26 (19)	44	35	46 (20)	53	30		45 (38)		
$m(3^3P_1)$-$m(3^3P_0)$	60		54 (46)	58	18	69 (25)	81	47		63 (69)		

Table 4. Complete mass spectra (in GeV). (LP = linear potential model, SP = screened potential model, NR = non-relativistic and RE = relativistic,).

state		this	expt.	other works									
$n^{2S+1}L_J$	J^P	work	[4]	LP(SP) [79]	Ref. [108]	Ref. [114]	NR (GI) [73]	Ref. [76]	Ref. [75]	Ref. [110]	Ref. [111]	RE (NR) [112]	Ref. [113]
1^1S_0	0^{-+}	2.995	2.984	2.983 (2.984)	3.069	2.981	2.982 (2.975)	2.978	2.979	2.980	2.979	2.992 (2.982)	2.97
1^3S_1	1^{--}	3.094	3.097	3.097 (3.097)	3.097	3.096	3.090 (3.098)	3.088	3.097	3.097	3.096	3.094 (3.090)	3.10
2^1S_0	0^{-+}	3.606	3.639	3.635 (3.637)	3.659	3.635	3.630 (3.623)	3.647	3.623	3.597	3.588	3.625 (3.630)	3.62
2^3S_1	1^{--}	3.649	3.686	3.679 (3.679)	3.670	3.686	3.672 (3.676)	3.685	3.673	3.686	3.686	3.668 (3.672)	3.68
3^1S_0	0^{-+}	4.000		4.048 (4.004)	4.063	3.989	4.043 (4.064)	4.058	3.991	4.014	3.991	4.029 (4.043)	4.06
3^3S_1	1^{--}	4.036	4.039	4.078 (4.030)	4.072	4.039	4.072 (4.100)	4.087	4.022	4.095	4.088	4.059 (4.072)	4.10
4^1S_0	0^{-+}	4.328		4.388 (4.264)	4.403	4.401	4.384 (4.425)	4.391	4.250			4.332 (4.388)	
4^3S_1	1^{--}	4.362	4.421	4.412 (4.281)	4.409	4.427	4.406 (4.450)	4.411	4.273	4.433		4.356 (4.406)	4.45
5^1S_0	0^{-+}	4.622		4.690 (4.459)	4.705	4.811			4.446			4.639 (4.685)	
5^3S_1	1^{--}	4.654	4.643	4.711 (4.472)	4.711	4.837			4.463			4.661 (4.704)	
6^1S_0	0^{-+}	4.893			4.983	5.155			4.595			4.893 (4.960)	
6^3S_1	1^{--}	4.925			4.988	5.167			4.605			4.912 (4.977)	
1^3P_0	0^{++}	3.457	3.415	3.415 (3.415)	3.440	3.413	3.424 (3.445)	3.366	3.433	3.416	3.424	3.472 (3.424)	3.44
1^3P_1	1^{++}	3.523	3.511	3.516 (3.521)	3.503	3.511	3.505 (3.510)	3.518	3.510	3.508	3.510	3.543 (3.505)	3.51
1^1P_1	1^{+-}	3.534	3.525	3.522 (3.526)	3.526	3.525	3.516 (3.517)	3.527	3.519	3.527	3.526	3.544 (3.516)	3.52
1^3P_2	2^{++}	3.556	3.556	3.552 (3.553)	3.550	3.555	3.556 (3.550)	3.559	3.554	3.558	3.556	3.584 (3.549)	3.55
2^3P_0	0^{++}	3.866	3.918	3.869 (3.848)	3.862	3.870	3.852 (3.916)	3.843	3.842	3.844	3.854	3.885 (3.852)	3.92
2^3P_1	1^{++}	3.925	3.872	3.937 (3.914)	3.921	3.906	3.925 (3.953)	3.935	3.901	3.940	3.929	3.951 (3.925)	3.95
2^1P_1	1^{+-}	3.936	3.887	3.940 (3.916)	3.944	3.926	3.934 (3.956)	3.942	3.908	3.961	3.945	3.951 (3.934)	3.96
2^3P_2	2^{++}	3.956	3.927	3.967 (3.937)	3.967	3.949	3.972 (3.979)	3.973	3.937	3.994	3.972	3.994 (3.965)	3.98
3^3P_0	0^{++}	4.197		4.230 (4.146)	4.212	4.301	4.202 (4.292)	4.208	4.131			4.219 (4.202)	
3^3P_1	1^{++}	4.257	4.273	4.284 (4.192)	4.270	4.319	4.271 (4.317)	4.299	4.178			4.283 (4.271)	
3^1P_1	1^{+-}	4.269		4.285 (4.193)	4.292	4.337	4.279 (4.318)	4.310	4.184			4.283 (4.279)	
3^3P_2	2^{++}	4.290		4.310 (4.311)	4.314	4.354	4.317 (4.337)	4.352	4.208			4.328 (4.309)	
1^3D_1	1^{--}	3.799	3.773	3.787 (3.792)	3.759	3.783	3.785 (3.819)	3.809	3.787	3.804	3.798	3.830 (3.785)	3.82
1^3D_2	2^{--}	3.805	3.822	3.807 (3.807)	3.787	3.795	3.800 (3.838)	3.820	3.798	3.824	3.813	3.841 (3.800)	3.84
1^1D_2	2^{-+}	3.802		3.806 (3.805)	3.799	3.807	3.799 (3.879)	3.815	3.796	3.824	3.811	3.837 (3.799)	3.84
1^3D_3	3^{--}	3.801		3.811 (3.808)	3.823	3.813	3.806 (3.849)	3.813	3.799	3.831	3.815	3.844 (3.805)	3.84
2^3D_1	1^{--}	4.145	4.191	4.144 (4.095)	4.119	4.150	4.142 (4.194)	4.154	4.089	4.164		4.174 (4.141)	4.19
2^3D_2	2^{--}	4.152		4.165 (4.109)	4.148	4.190	4.158 (4.208)	4.169	4.100	4.189		4.187 (4.158)	4.21
2^1D_2	2^{-+}	4.150		4.164 (4.108)	4.160	4.196	4.158 (4.208)	4.165	4.099	4.191		4.183 (4.158)	4.21
2^3D_3	3^{--}	4.151		4.172 (4.112)	4.185	4.220	4.167 (4.217)	4.166	4.103	4.202		4.195 (4.165)	4.22
3^3D_1	1^{--}	4.448		4.456 (4.324)	4.437	4.448		4.502	4.317	4.477		4.470 (4.455)	4.52
3^3D_2	2^{--}	4.456		4.478 (4.337)	4.466	4.456		4.524	4.327			4.485 (4.472)	
3^1D_2	2^{-+}	4.455		4.478 (4.336)	4.478	4.455		4.524	4.326			4.480 (4.472)	
3^3D_3	3^{--}	4.457		4.486 (4.340)	4.503	4.457		4.527	4.331			4.497 (4.481)	

$$\Gamma(n^3P_0\to\gamma\gamma)=\frac{27e_Q^4\alpha^2|R'_{nP}(0)|^2}{m_Q^4}\left(1+\frac{0.2\alpha_s}{\pi}\right), \quad (25)$$

$$\Gamma(n^3P_2\to\gamma\gamma)=\frac{36e_Q^4\alpha^2|R'_{nP}(0)|^2}{5m_Q^4}\left(1-\frac{16\alpha_s}{3\pi}\right), \quad (26)$$

$$\Gamma(n^3S_1\to3\gamma)=\frac{4(\pi^2-9)e_Q^6\alpha^3|R_{nS}(0)|^2}{3\pi m_Q^2}\left(1-\frac{12.6\alpha_s}{\pi}\right). \quad (27)$$

2.4.3 Decay into gluons

The annihilation decay of the charmonium states into two or three gluons, as well as into gluons with photons and light quarks, without and/or with radiative QCD correction, are given by [101–103, 105]:

$$\Gamma(n^1S_0\to gg)=\frac{2\alpha_s^2|R_{nS}(0)|^2}{3m_Q^2}\left(1+\frac{4.8\alpha_s}{\pi}\right), \quad (28)$$

$$\Gamma(n^3P_0\to gg)=\frac{6\alpha_s^2|R'_{nP}(0)|^2}{m_Q^4}, \quad (29)$$

$$\Gamma(n^3P_2\to gg)=\frac{8\alpha_s^2|R'_{nP}(0)|^2}{5m_Q^4}, \quad (30)$$

$$\Gamma(n^1D_2\to gg)=\frac{2\alpha_s^2|R''_{nD}(0)|^2}{3\pi m_Q^6}, \tag{31}$$

$$\Gamma(n^3S_1\to 3g)=\frac{10(\pi^2-9)\alpha_s^3|R_{nS}(0)|^2}{81\pi m_Q^2}\left(1-\frac{3.7\alpha_s}{\pi}\right), \tag{32}$$

$$\Gamma(n^1P_1\to 3g)=\frac{20\alpha_s^3|R'_{nP}(0)|^2}{9\pi m_Q^4}\ln(m_Q\langle r\rangle). \tag{33}$$

$$\Gamma(n^3D_1\to 3g)=\frac{760\alpha_s^3|R''_{nP}(0)|^2}{81\pi m_Q^6}\ln(4m_Q\langle r\rangle), \tag{34}$$

$$\Gamma(n^3D_2\to 3g)=\frac{10\alpha_s^3|R''_{nP}(0)|^2}{9\pi m_Q^4}\ln(4m_Q\langle r\rangle), \tag{35}$$

$$\Gamma(n^3D_3\to 3g)=\frac{40\alpha_s^3|R''_{nP}(0)|^2}{9\pi m_Q^6}\ln(4m_Q\langle r\rangle), \tag{36}$$

$$\Gamma(n^3S_1\to \gamma gg)=\frac{8(\pi^2-9)e_Q^2\alpha\alpha_s^2|R_{nS}(0)|^2}{9\pi m_Q^2}\left(1-\frac{6.7\alpha_s}{\pi}\right), \tag{37}$$

$$\Gamma(n^3P_1\to q\bar{q}+g)=\frac{8\eta_f\alpha_s^3|R'_{nP}(0)|^2}{9\pi m_Q^4}\ln(m_Q\langle r\rangle). \tag{38}$$

The calculated annihilation decay widths of charmonium are listed in Tables 7 to 13.

Table 5. Electric dipole (E1) transition widths of $c\bar{c}$ mesons. (LP = linear potential model, SP = screened potential model, NR = non-relativistic and RE = relativistic). E_γ is in MeV and Γ in keV.

transition		this work		expt. [4]	other works									
initial	final	E_γ	Γ	Γ	Ref. [75]	Ref. [111]	Ref. [115]	Ref. [73] NR(GI)	Ref. [116]	Ref. [117]	Ref. [77]	Ref. [76]	Ref. [79] LP(SP)	Ref. [112] RE(NR)
1^3P_2	1^3S_1	432.31	233.85	406±31	309	327	383	424 (313)	315	315		405	327(338)	437.5(424.5)
1^3P_1	1^3S_1	402.92	189.86	320±25	244	265	361	314 (239)	241	242		341	269 (278)	329.5(319.5)
1^1P_1	1^1S_0	497.67	357.83		323	560	671	498 (352)	482	482		473	361 (373)	570.5(490.3)
1^3P_0	1^3S_1	344.13	118.29	131±14	117	121	264	152 (114)	120	120		104	141(146)	159.2(154.5)
2^3S_1	1^3P_2	91.58	7.07	26±1.5	34	18.2		38 (24)	30.1	29	28.6	39	36(44)	35.5 (37.9)
2^3S_1	1^3P_1	123.46	10.39	27.9±1.5	36	22.9		54 (29)	42.8	41	33.0	38	45(48)	50.9 (54.2)
2^3S_1	1^1P_1	112.88	7.94		104									
2^3S_1	1^3P_0	186.43	11.93	29.8±1.5	25	26.3		63 (26)	47	46	28.8	29	27(26)	58.8 (62.6)
2^1S_0	1^3P_1	82.19	9.20											
2^1S_0	1^1P_1	71.49	6.05			6.2		49 (36)	35.1	35.1		56	49 (52)	45.2 (49.9)
1^3D_3	1^3P_2	237.31	237.51		323	156	432	272 (296)	402			302		397.7(271.1)
1^3D_2	1^3P_2	241.19	62.34		55	59	131	64 (66)	69.5	56		82	79(82)	96.52(64.06)
1^3D_2	1^3P_1	271.75	89.18		208	215	423	307 (268)	313	260		301	281(291)	438.2(311.2)
1^3D_1	1^3P_2	235.48	6.45	<21	4.6	6.9	15.2	4.9 (3.3)	3.88	3.7	3.3	8.1	5.4 (5.7)	4.73(4.86)
1^3D_1	1^3P_1	266.10	139.52	70±17	93	135	246	125 (77)	99	94	89.7	153	115 (111)	122.8(126.2)
1^3D_1	1^3P_0	326.57	343.87	172±30	197	355	448	403 (213)	299	287	221.7	362	243 (232)	394.6(405.4)
2^3P_2	2^3S_1	295.70	281.93		100		164	304 (207)				264		377.1(287.5)
2^3P_1	2^3S_1	266.71	206.87		60		174	183 (183)				234		246.0(185.3)
2^1P_1	2^1S_0	315.84	343.55		108		333	280 (218)				274		349.8(272.9)
2^3P_0	2^3S_1	210.86	102.23		44		112	64 (135)				83		108.3(65.3)
2^3P_2	1^3D_3	152.16	33.27					88 (29)				76		60.67(78.69)
2^3P_2	1^3D_2	148.18	5.49					17 (5.6)				10		11.48(15.34)
2^3P_2	1^1D_2	151.21	5.83											
2^3P_2	1^3D_1	154.03	0.41					1.9 (1.0)				0.64		2.31(1.67)
2^3P_1	1^3D_1	123.91	5.35					22 (21)				11		31.15(21.53)
2^3P_0	1^3D_1	65.87	3.21					13 (51)				1.4		33.24(13.55)

Table 6. Magnetic dipole (M1) transition widths. (LP = linear potential model, SP = screened potential model, NR = non-relativistic and RE = relativistic). E_γ is in MeV and Γ in keV.

transition		this work		expt. [4]	other works								
initial	final	E_γ	Γ	Γ	Ref. [111]	Ref. [115]	NR(GI) [73]	Ref. [116]	Ref. [117]	Ref. [77]	Ref. [76]	LP(SP) [79]	RE(NR) [112]
1^3S_1	1^1S_0	97	1.647	1.58±0.37	1.05	2.01	2.9 (2.4)	1.960	1.92	2.0	2.2	2.39 (2.44)	2.765 (2.752)
2^3S_1	2^1S_0	42	0.135	0.21±0.15	0.99	0.20	0.21 (0.17)	0.140	0.04	0.2	0.096	0.19 (0.19)	0.198 (0.197)
3^3S_1	3^1S_0	36	0.082			0.012	0.046 (0.067)			0.0046	0.044	0.051 (0.088)	0.023 (0.044)
2^3S_1	1^1S_0	595	69.57	1.24±0.29	0.95		4.6 (9.6)	0.926	0.91		3.8	8.08 (7.80)	3.370 (4.532)
2^1S_0	1^3S_1	476	35.72		1.12		7.9 (5.6)	0.538		7.2	6.9	2.64 (2.29)	5.792 (7.962)
1^3P_2	1^3P_0	97	1.638										
1^3P_2	1^3P_1	33	0.189										
1^3P_2	1^1P_1	22	0.056										
1^1P_1	1^3P_0	76	0.782										

Table 7. Leptonic decay widths ($\psi \to \Gamma_{e^+e^-}$ in keV).

state	this work		expt. [4]	other works								
	$\Gamma_{l^+l^-}$	$\Gamma^{cf}_{l^+l^-}$		Ref. [118]	Refs. [106, 119]	Ref. [75]	Ref. [120]	Ref. [110]	Ref. [73]	Ref. [77]	Ref. [76]	Ref. [61]
J/ψ	8.335	3.623	5.55±0.14±0.02	3.112	6.847 (2.536)	11.8 (6.60)	4.080	4.28	12.13	3.93	6.0(3.3)	5.63
$\psi(2S)$	2.496	1.085	2.33±0.07	2.197	3.666 (1.358)	4.29 (2.40)	2.375	2.25	5.03	1.78	2.2(1.2)	2.19
$\psi(3S)$	1.722	0.748	0.86±0.07	1.701	2.597 (0.962)	2.53 (1.42)	0.835	1.66	3.48	1.11	1.8(0.98)	1.20
$\psi(4S)$	1.378	0.599	0.58±0.07		2.101 (0.778)	1.73 (0.97)		1.33	2.63	0.78	1.3(0.70)	0.63
$\psi(5S)$	1.168	0.508			1.701 (0.633)	1.25 (0.70)				0.57		0.24
$\psi(6S)$	1.017	0.442				0.88 (0.49)				0.42		
1^3D_1	0.261	0.113	0.262±0.018	0.275	0.096	0.055 (0.031)		0.09	0.056	0.22	0.079(0.044)	
2^3D_1	0.381	0.166	0.48±0.22	0.223	0.112	0.066 (0.037)		0.16	0.096	0.30	0.13(0.073)	
3^3D_1	0.485	0.211				0.079 (0.044)				0.33		

Table 8. Two-photon decay widths without and with correction factor (in keV).

state	this work		expt. [4]	other works										
	$\Gamma_{\gamma\gamma}$	$\Gamma^{cf}_{\gamma\gamma}$		Ref. [118]	Ref. [107]	Refs. [106, 119]	Ref. [75]	Ref. [121]	Ref. [122]	Ref. [93]	Ref. [123]	Ref. [120]	Ref. [76]	Ref. [124]	Ref. [122]
$\eta_c(1S)$	10.351	6.621	5.1±0.4	6.96	7.918	6.68	8.5	5.09	3.5	7.18	7.14	4.252	7.5	5.5	3.5
$\eta_c(2S)$	4.501	2.879	2.15±0.6	10.45	5.789	5.08	2.4	2.63	1.38	1.71	4.44	3.306	2.9	1.8	1.38
$\eta_c(3S)$	3.821	2.444		1.03	0.299	4.53	0.88		0.94	1.21		1.992	2.5		
$\eta_c(4S)$	3.582	2.291							0.73				1.8		
$\eta_c(5S)$	3.460	2.213							0.62						
$\eta_c(6S)$	3.378	2.161													
1^3P_0	1.973	2.015	2.36±0.35	13.43		2.62	2.5	2.02	1.39	3.28			10.8	2.9	1.39
2^3P_0	2.299	2.349		2.67			1.7		1.11				6.7	1.9	1.11
3^3P_0	2.714	2.773					1.2		0.91				6.5		
1^3P_2	0.526	0.229	0.53±0.03	1.72		0.25	0.31	0.46	0.44				0.27	0.50	0.44
2^3P_2	0.613	0.267		0.343			0.23		0.48				0.39	0.52	0.48
3^3P_2	0.724	0.315					0.17		0.014				0.66		

Table 9. Three-photon decay widths (in eV).

state	this work		expt. [4]
	$\Gamma_{\gamma\gamma\gamma}$	$\Gamma^{cf}_{\gamma\gamma\gamma}$	
J/ψ	4.41691	3.94748	1.08±0.032
$\psi(2S)$	1.83911	1.64365	
$\psi(3S)$	1.55252	1.38752	
$\psi(4S)$	1.45187	1.29756	
$\psi(5S)$	1.40027	1.25145	
$\psi(6S)$	1.36564	1.2205	

Table 10. Three-gluon decay widths (in keV) .

state	this work		expt. [4]	other works	
	Γ_{ggg}	Γ^{cf}_{ggg}		Ref. [117]	Ref. [31] MeV
J/ψ	442.669	269.059	59.55±0.18	52.8±5	
$\psi(2S)$	184.318	112.031	31.38±0.85	23±2.6	
$\psi(3S)$	155.596	94.5727			
$\psi(4S)$	145.508	88.4413			
$\psi(5S)$	140.337	85.2984			
$\psi(6S)$	136.866	83.1888			
1^1P_1	285.127			720±320	
2^1P_1	420.078				1.29
3^1P_1	558.78				
1^3D_1	189.367			216	1.15
2^3D_1	359.346				
3^3D_1	556.588				
1^3D_2	53.8761			36	0.08
2^3D_2	102.236				
3^3D_2	158.353				
1^3D_3	89.7001			102	0.18
2^3D_3	170.217				
3^3D_3	263.647				

Table 11. Two-gluon decay widths (in MeV).

state	this work		expt. [4]	other works					
	Γ_{gg}	Γ^{cf}_{gg}		Ref. [118]	Ref. [107]	Refs. [106, 119]	Ref. [121]	Ref. [123]	Ref. [117]
$\eta_c(1S)$	24.249	36.587	28.6±2.2	28.60	13.070	32.44	15.70	19.6	17.4±2.8
$\eta_c(2S)$	10.545	15.910	14±7	42.90	9.534	24.64	8.10	12.1	8.3±1.3
$\eta_c(3S)$	8.952	13.507		4.26	4.412	21.99			
$\eta_c(4S)$	8.392	12.662							
$\eta_c(5S)$	8.106	12.230							
$\eta_c(6S)$	7.914	11.941							
1^3P_0	4.621	9.274	10±0.6	47.76		15.67	4.68		14.3±3.6
2^3P_0	5.386	10.810		9.50					
3^3P_0	6.357	12.758							
1^3P_2	1.232	0.945	1.97±0.11	5.27		1.46	1.72		1.71±0.21
2^3P_2	1.436	1.101		1.04					
3^3P_2	1.695	1.300							
1^1D_2	12.460 (KeV)								110 (KeV)
2^1D_2	21.679 (KeV)								
3^1D_2	31.757 (KeV)								

Table 12. $n^3S_1 \to \gamma gg$ decay widths.

state	this work		expt. [4]
	$\Gamma_{\to\gamma gg}$/keV	$\Gamma^{cf}_{\to\gamma gg}$/keV	
J/ψ	31.0421	8.99657	8.18±0.25
$\psi(2S)$	12.9253	3.74599	2.93±0.16
$\psi(3S)$	10.9111	3.16224	
$\psi(4S)$	10.2037	2.95723	
$\psi(5S)$	9.8411	2.85214	
$\psi(6S)$	9.59771	2.7816	

Table 13. $n^3P_1 \to q\overline{q}+g$ decay widths.

state	this work $\Gamma_{q\overline{q}+g}$/keV
1^3P_1	342.152
2^3P_1	504.093
3^3P_1	670.536

3 Results and discussion

In the framework of the Cornell potential with a Gaussian wave function and relativistic correction of the Hamiltonian, comprised of a $\mathcal{O}(1/m)$ rectification in the potential energy term and elaboration of the kinetic energy term up to $\mathcal{O}(\boldsymbol{p}^{10})$, we have studied the mass spectra of charmonium states. We have calculated the center of weight masses (value of Hamiltonian yields) for the nS ($n\leqslant 6$), nP and nD ($n\leqslant 3$) charmonium states, as shown in Table 2. We observe that the Hamiltonian yields for nS ($n\leqslant 3$) and nP and nD ($n\leqslant 3$) are in accordance with experimental measurements as well as the values predicted by other theoretical models, whereas the results

for nS $(4\leqslant n\leqslant 6)$ are underestimated or overestimated compared to the results of other theoretical models.

The calculated masses of the charmonium states are graphically represented in Fig. 1 and listed in Table 4 with the experimentally observed results. After addition of the spin hyperfine interaction to the fixed spin average mass for the ground state, we obtain the pseudoscalar state mass η_c (2995 MeV) and vector state mass J/ψ (3094 MeV). The estimated mass of 2^1S_0 (3606 MeV) is 33 MeV lower than the experimentally observed mass, whereas the mass of $3^3S_1(4036)$ is in accordance with the mass given by the PDG [4] and by other model estimates [75, 79, 114]. Our calculated mass for 5^3S_1 (4654 MeV) is 11 MeV higher than the value quoted by the PDG [4] and in accordance with the mass estimated by other models [110, 112]. We have assigned $X(4660)$ to the 5^3S_1 state of charmonium. The estimated masses of the 6^3S_0 (4893 MeV) and 6^3S_1 (4925 MeV) states agree with the masses estimated by other models [112].

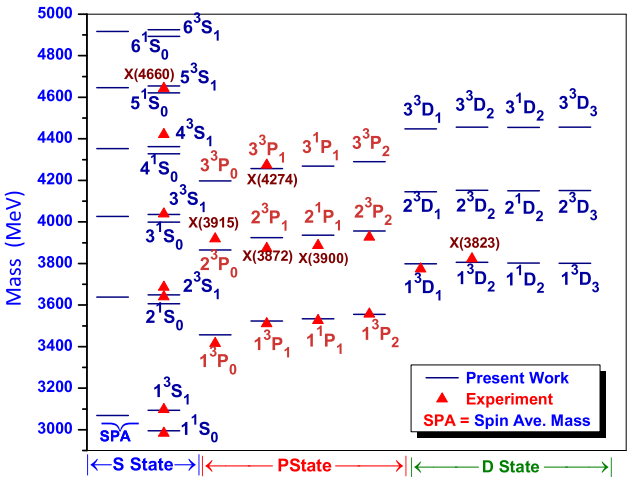

Fig. 1. (color online) Mass spectrum.

The P-wave states, 1^3P_1 with predicted mass 3511 MeV, 1^1P_1 with predicted mass 3525 MeV and 2^3P_2 with predicted mass 3556 MeV, are in good agreement with the experimentally observed values [4].

We have assigned the newly observed charmonium-like state $X(3900)$ to the 2^1P_1 (3936 MeV) and the state $X(3872)$ to the 2^3P_1 (3925 MeV). The masses predicted for the states 2^1P_1 (3936 MeV) and 2^3P_1 (3925 MeV) are in good agreement with the masses predicted by other models [65, 73, 76, 79, 108, 112, 114]. We assign $X(3872)$ as a candidate for the 2^3P_1 state, with well established quantum numbers, although its interpretation as a molecular state [125, 126] was questioned in Ref. [127], while Ref. [128] interpreted it as a virtual state.

Reference [129] predicts X(3872) to be a tetraquarks with a mass difference related to m_u–m_d. Reference [130] described the structures of the $X(3872)$ and $X(3915)$ states as $(cq)[\bar{c}\bar{q}]$ tetraquarks with help of the light-front Hamiltonian QCD (LFHQCD) approach.

We have also assigned the charmonium-like states $X(3915)$ and $X(4274)$ to the 2^3P_0 (3866 MeV) and 3^3P_1(4257 MeV) states respectively. To consider $X(3915)$ as the 2^3P_0 state is still problematic, as was also pointed out in Ref. [79, 131] and the references therein. In Ref. [131–133], the authors suggest the $X(3915)$ as the 2^3P_0 state faces the following problems. First, scalar mesons should be the open-flavor modes for the dominant decay channels, above the corresponding thresholds. $X(3915)$ should therefore couple in an S-wave and the $D\bar{D}$ channel, although this has not been observed in the $D\bar{D}$ channel. Second, the mass splitting between the state 1^3P_2 and 1^3P_0 is 141 MeV, while the mass splitting between the relatively well determined $X(3930)$ as the 2^3P_2 state and $X(3915)$ as the 2^3P_0 state is 9 MeV, which is too small for the hyperfine splitting.

We observed that new charmonium-like states $X(4140)$ and $X(4274)$ with quantum numbers $J^{PC}=1^{++}$ are good candidates for the 3^3P_1 state within the screened potential model and linear potential model respectively. However, none of the models can give $J^{PC}=1^{++}$ charmonium state masses 4147 MeV and 4273 MeV at the same time, which may indicate the exotic nature of $X(4140)$ and/or $X(4274)$, which was also pointed out in Ref. [79].

The predicted masses for the 1^3D_1 (3799 MeV), 1^3D_2 (3805 MeV) and 2^3D_1 (4145 MeV) states are in accordance with the experimentally observed results [4] as well as in good agreement with other model predictions [65, 73, 75, 76, 79, 112, 114]. The estimated masses of charmonium using our model are overall in agreement (with a few MeV difference) with experimentally observed values. It is found that states with a mass of $M<4.1$ GeV are in good agreement with other theoretical estimates.

Table 3 shows the hyperfine splittings for S wave states and fine splittings for some P wave states. For comparison, the experimental data from the PDG [4] and predictions with other theoretical models are also listed. The predicted hyperfine splittings up to the $2S$ states are in agreement with the world average data [4] and predictions with other theoretical models. The hyperfine splittings for the $3S$ to $6S$ states have different values in different theoretical models. By comparing our predicted results with other theoretical models, we observe that the masses of the low-lying nS $(n\leqslant 2)$, nP, and nD $(n=1)$ charmonium states have less difference, whereas the masses of the higher charmonium states $nS\,(n\geqslant 3)$, $nP, nD\,(n\geqslant 2)$ have considerable differences.

The estimated pseudoscalar and vector decay constants, $f_P(f_{Pcor})$ and $f_V(f_{Vcor})$ respectively, without and with QCD corrections, are shown in Table 1. They are in agreement with the experimental results as well as other theoretical model estimates.

The calculated radiative E1 and M1 dipole transitions widths are shown in Tables 5 and 6. We calculate the E1 transition of $\Gamma[1P\to(1S)\gamma]$, $\Gamma[2S\to(1P)\gamma]$, $\Gamma[1D\to(1P)\gamma]$, $\Gamma[2P\to(2S)\gamma]$ and $\Gamma[2P\to(1D)\gamma]$ using the masses predicted by our model. Our calculated E1 transitions for $\Gamma[1P\to(1S)\gamma]$ and $\Gamma[2S\to(1P)\gamma]$ are lower than the experimental results as well as other theoretical estimates, whereas for $\Gamma[1D\to(1P)\gamma]$, $\Gamma[2P\to(2S)\gamma]$ and $\Gamma[2P\to(1D)\gamma]$ transition, our results are in agreement with the estimates of other theoretical models. Our predictions for $\Gamma[1^3D_1\to(1^3P_1)\gamma]$ and $\Gamma[1^3D_1\to(1^3P_0)\gamma]$ are almost double that of the PDG average data [4], while our prediction of $\Gamma[1^3D_1\to(1^3P_2)\gamma]$ is in agreement with the PDG average data [4] as well as the values predicted by other models.

We also calculate the M1 transition of the low-lying $1S$, $2S$ and $3S$ states as well as the 1P states. Our predictions for $\Gamma[1^3S_1\to(1^1S_0)\gamma]$ and $\Gamma[2^3S_1\to(2^1S_0)\gamma]$ are in agreement with the PDG average data [4], while our prediction for $\Gamma[2^3S_1\to(1^1S_0)\gamma]$ is much higher than the PDG average data [4]. Gang Li and Qiang Zhao [134, 135] studied intermediate meson loop contributions to $1^3S_1,2^3S_1\to\gamma2^1S_0,(\gamma1^1S_0)$ apart from the dominant M1 transitions in an effective Lagrangian approach. Their results showed that the IML contributions are relatively small but play a crucial role. Radiative decay widths, including the M1 in the GI model and intermediate hadronic loops, are 1.59 keV for $1^3S_1\to\gamma2^1S_0$ and 0.032(0.86) keV for $2^3S_1\to\gamma2^1S_0(\gamma1^1S_0)$ [134]. Results including the M1 transition amplitude of the GI model and IML transitions are 1.58 ± 0.37 keV for $1^3S_1\to\gamma2^1S_0$ and 0.08 ± 0.03 $(2.78^{+2.65}_{-1.75})$ keV for $2^3S_1\to\gamma2^1S_0(\gamma1^1S_0)$ [135].

Our prediction for $\Gamma[3^3S_1\to(3^1S_0)\gamma]$ is in agreement with the other theoretical model predictions, while the prediction for $\Gamma[2^1S_0\to(1^3S_1)\gamma]$ is higher than predictions by other theoretical models. The various models have different estimates for the E1 and M1 transitions, which may be due to the models having different parameters or to treatments in the relativistic corrections. The E1 and M1 transitions in general are strongly model dependent and more studies are required in experiments as well as theory.

We estimate the partial decay widths Γ and Γ^{cf} (with QCD correction factor) of annihilation processes, using the masses predicted by our potential model and the radial wave function at the origin, for e^+e^-, two-photon, three-photon, two-gluon, three-gluon, γgg and $q\bar{q}+g$ processes. The results are tabulated in Tables 7–13 and are compared with experimental results from the PDG [4] as well as other theoretically calculated estimates.

Our estimated leptonic decay widths without QCD correction for J/ψ, ψ(2S), ψ(3S) and ψ(4S) are higher than the experimentally observed leptonic decay widths. After QCD correction, the estimated leptonic decay widths are 1.93 keV, 1.24 keV, 0.11 keV and 0.019 keV less than the experimental results for the J/ψ, ψ(2S), ψ(3S) and ψ(4S) states respectively. Also, our estimated leptonic decay width with QCD correction for the n^3D_1 state is much lower than the experimental result.

Our estimated two-photon and two-gluon decay widths with QCD correction for the $\eta_c(nS)$, n^3P_0 and n^3P_2 states are in accordance with the experimentally observed results as well as with the other theoretical estimates. Our estimated three-photon decay width with QCD correction for J/ψ is lower than the experimentally observed result, while the estimated three-gluon decay widths with QCD correction for the J/ψ and ψ(2S) states are higher than the experimentally observed result as well as other theoretical estimates.

Our estimated γgg decay widths with QCD correction for the J/ψ and ψ(2S) states are in accordance with the experimentally observed results. We have also computed the $q\bar{q}+g$ decay width for the n^3P_1 states. We observe that the radiative QCD corrections modify the theoretical predictions considerably and bring the estimated result close to the experimental data. We also observe that the estimated values of annihilation decay width by various models show wide variation. Due to the considerable uncertainties which arise from the wave function dependence of the model and possible relativistic as well as QCD radiative corrections, we would like to mention that formulas used for calculation of annihilation decay width should be regarded as estimates of the partial widths rather than precise predictions.

3.1 Regge trajectories

We plot the Regge trajectories for the (n,M^2) and (J,M^2) planes with the help of masses estimated by our potential model. The "daughter" trajectories are the trajectories with the same value of J and differ by a quantum number corresponding to the radial quantum number. The masses of the "daughter" trajectories are higher than those of the leading trajectory with given quantum numbers. The linearity of Regge trajectories represents a reflection of strong forces between quarks at large distances (color confinement).

The Regge trajectories in the (J,M^2) plane with $(P=(-1)^J)$ $(J^P=1^-,2^+,3^-)$ natural and $(P=(-1)^{J-1})$ $(J^P=0^-,1^+,2^-)$ unnatural parity are depicted in Figs. 2–3. In the figures, the charmonium masses estimated by our model are represented by the solid triangles and experimentally available masses with the

corresponding charmonium name are represented by hollow squares. The Regge trajectories for $n_r=n-1$ principal quantum number in the (n_r,M^2) plane are shown in Figs. 4 and 5.

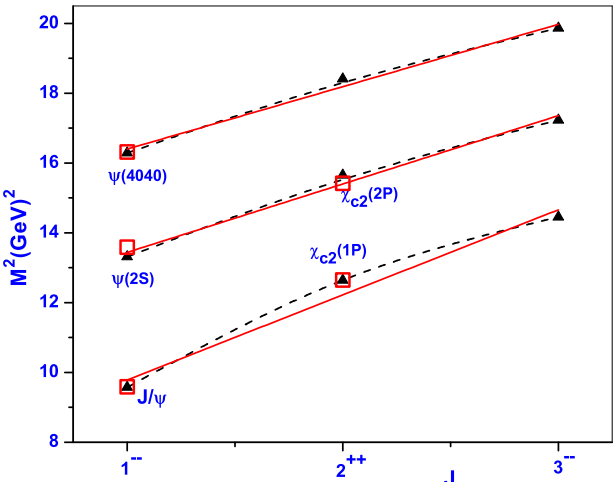

Fig. 2. (color online) Regge trajectory $(M^2\to J)$ with natural parity.

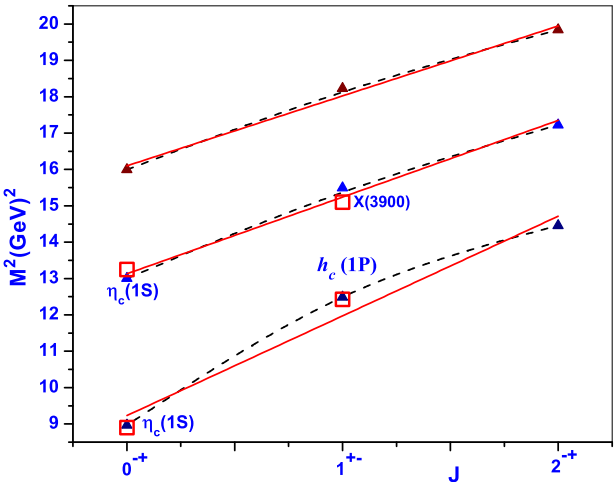

Fig. 3. (color online) Regge trajectory $(M^2\to J)$ with unnatural parity.

The following definitions are used to calculate the χ^2 fitted slopes $(\alpha,\ \beta)$ and the intercepts $(\alpha_0,\ \beta_0)$ [83, 84]:

$$J=\alpha M^2+\alpha_0, \tag{39}$$

$$n_r=\beta M^2+\beta_0. \tag{40}$$

The calculated slopes and intercepts are tabulated in Tables 14, 15, and 16). The estimated masses of the charmonium fit well to the (n,M^2) and (J,M^2) planes trajectories. The daughter trajectories, which involve both radially and orbitally excited states, turn out to be almost linear, equidistant and parallel whereas the parent Regge trajectories, which start from the ground states, exhibit nonlinear behavior in the lower mass region in both planes.

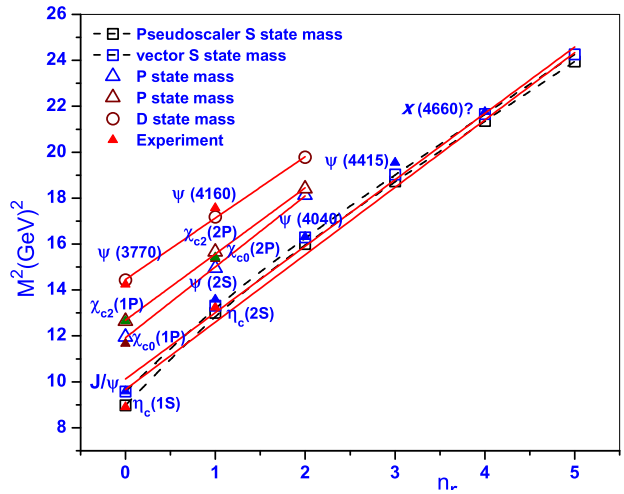

Fig. 4. (color online) Regge trajectory $(M^2\to n_r)$ for the pseudoscalar and vector S state and excited P and D state masses.

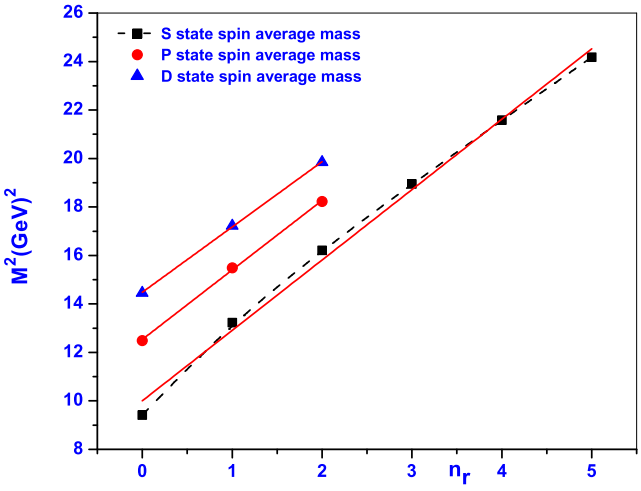

Fig. 5. (color online) Regge trajectory $(M^2\to n_r)$ for the S-P-D states center of weight mass.

The linearity of the Regge trajectories depends on the quark masses, as the orbital momentum ℓ of the state is proportional to its mass: $\ell=\alpha M^2(\ell)+\alpha(0)$, where the slope α depends on the flavor content of the states lying on the corresponding trajectory. In the Regge phenomenology, the radial spectrum of heavy quarkonia typically leads to strong nonlinearities, in the framework of

the hadron string model [136].

Table 14. Slopes and intercepts of the (J, M^2) Regge trajectories with unnatural and natural parity.

parity	trajectory	$\alpha/(\mathrm{GeV}^{-2})$	α_0
unnatural	Parent	0.355±0.058	−3.252±0.706
	first daughter	0.471±0.038	−6.164±0.576
	second daughter	0.518±0.032	−8.319±0.570
natural	parent	0.401±0.060	−2.902±0.746
	first daughter	0.504±0.057	−5.764±0.877
	second daughter	0.553±0.059	−8.057±1.081

Table 15. Slopes and intercepts for the (n_r, M^2) Regge trajectories.

meson	J^P	$\beta/(\mathrm{GeV}^{-2})$	β_0
η_c	0^{-+}	0.341±0.017	−3.236±0.303
Υ	1^{--}	0.347±0.014	−3.463±0.252
χ_{c0}	0^{++}	0.324±0.006	−3.861±0.088
χ_{c1}	1^{++}	0.355±0.007	−4.441±0.112
h_c	1^{+-}	0.346±0.009	−4.399±0.138
χ_{c2}	2^{++}	0.345±0.012	−4.284±0.183
$\psi(^3D_1)$	1^{--}	0.374±0.006	−5.406±0.104
$\psi(^3D_2)$	2^{--}	0.377±0.009	−5.473±0.159
$\psi(^1D_2)$	2^{-+}	0.371±0.006	−5.372±0.101
$\psi(^3D_3)$	3^{--}	0.369±0.006	−5.344±0.100

Table 16. Slopes and intercepts of (n_r, M^2) Regge trajectory for center of weight mass.

trajectory	$\beta/(\mathrm{GeV}^{-2})$	β_0
S State	0.342±0.012	−3.413±0.226
P State	0.348±0.009	−4.36±0.1464
D State	0.371±0.006	−5.372±0.101

4 Conclusion

We can conclude that the mass spectra of charmonium, Tables 2 and 4, investigated using a Cornell potential with relativistic correction to the Hamiltonian, are in accordance with the available experimental results as well as those predicted by the other theoretical models. The predicted pseudoscalar (f_{Pcor}) and the vector (f_{Vcor}) decay constants with QCD correction using our estimated charmonium masses are in accordance with experimental results as well as those predicted by other theoretical models.

We observe from the Regge trajectories in Figs. 2–5 that the experimental masses of the charmonium states are sitting nicely. In the mass region of the lowest excitations of charmonium, the slope of the trajectories decreases with increasing quark mass. The curvature of the trajectory near the ground state is due to the contribution of the color Coulomb interaction, which increases with mass. Hence, the Regge trajectories of the charmonium are basically nonlinear and exhibit nonlinear behavior in the lower mass region.

From a comparison of our estimated radiative (E1 and M1 dipole) transition widths with other theoretical estimations, we conclude that the various models have very different predictions for the E1 and M1 dipole transitions, which may be due to the different parameters and treatments used in the relativistic corrections in the model. The calculated E1 and M1 dipole transition widths using the masses and parameters estimated by our model are in agreement with other theoretical and experimental predictions. However, in most cases, more precise experimental measurements are required.

We also conclude from the calculated annihilation decay widths using the Van Royen-Weisskopf relation that the inclusion of QCD correction factors is helpful in bringing the estimated results closer to the experimental results. The various models show a wide variation in results for the annihilation decay widths, which may be resolved using the NRQCD (non-relativistic QCD) and pNRQCD (potential non-relativistic QCD) formalisms.

A. K. Rai acknowledges the financial support extended by the Department of Science of Technology, India under the SERB fast track scheme SR/FTP /PS-152/2012.

References

1 J.J. Aubert et al (E598), Phys. Rev. Lett., **33**: 1404 (1974)
2 J.E. Augustin et al (SLAC-SP-017), Phys. Rev. Lett., **33**: 1406 (1974)
3 N. Brambilla, S. Eidelman, B. Heltsley, R. Vogt, G. Bodwin et al, Eur. Phys. J. C, **71**: 1534 (2011)
4 C. Patrignani, P. D. Group, Chinese Physics C, **40**: 100001 (2016)
5 J. Siegrist et al, Phys. Rev. Lett., **36**: 700 (1976)
6 R. Brandelik et al (DASP), Phys. Lett. B, **76**: 361 (1978)
7 E. Eichten, K. Gottfried, T. Kinoshita, K. D. Lane, and T. M. Yan, Phys. Rev. D, **21**: 203 (1980)
8 R. Aaij et al (LHCb), Phys. Rev. Lett., **111**: 101805 (2013)
9 X. L. Wang et al (Belle), Phys. Rev. Lett., **99**: 142002 (2007)
10 G. Pakhlova et al (Belle), Phys. Rev. Lett., **101**: 172001 (2008)
11 P. A. Rapidis et al, Phys. Rev. Lett., **39**: 526 (1977)
12 W. Bacino et al, Phys. Rev. Lett., **40**: 671 (1978)
13 G. S. Abrams et al, Phys. Rev. D, **21**: 2716 (1980)
14 M. Ablikim et al (BES), Phys. Lett. B, **652**: 238 (2007)
15 V. V. Anashin et al, Phys. Lett. B, **711**: 292 (2012)
16 K. Abe et al (Belle), Phys. Rev. Lett., **98**: 082001 (2007)
17 P. Pakhlov et al (Belle), Phys. Rev. Lett., **100**: 202001 (2008)
18 W. Sreethawong, K. Xu, Y. Yan (2013), 1306.2780
19 Z. H. Wang, Y. Zhang, L. Jiang, T. H. Wang, Y. Jiang, and G. L. Wang, Eur. Phys. J. C, **77**(1): 43 (2017)

20 V. Bhardwaj et al (Belle), Phys. Rev. Lett., **111**(3): 032001 (2013)
21 M. Ablikim et al (BESIII), Phys. Rev. Lett., **115**(1): 011803 (2015)
22 S. K. Choi et al (Belle), Phys. Rev. Lett., **91**: 262001 (2003)
23 D. Acosta et al (CDF), Phys. Rev. Lett., **93**: 072001 (2004)
24 V.M. Abazov et al (D0), Phys. Rev. Lett., **93**: 162002 (2004)
25 B. Aubert et al (BaBar), Phys. Rev. D, **71**: 071103 (2005)
26 S.K. Choi et al, Phys. Rev. D, **84**: 052004 (2011)
27 T. Aaltonen et al (CDF), Phys. Rev. Lett., **103**: 152001 (2009)
28 B. Aubert et al (BaBar), Phys. Rev. D, **77**: 111101 (2008)
29 A. Abulencia et al (CDF), Phys. Rev. Lett., **98**: 132002 (2007)
30 M. Ablikim et al (BESIII), Phys. Rev. Lett., **112**(9): 092001 (2014)
31 T. Barnes, S. Godfrey, Phys. Rev. D, **69**: 054008 (2004)
32 S. K. Choi et al (Belle Collaboration), Phys. Rev. Lett., **94**: 182002 (2005)
33 P. del Amo Sanchez et al (BaBar), Phys. Rev. D, **82**: 011101 (2010)
34 J.P. Lees et al (BaBar), Phys. Rev. D, **86**: 072002 (2012), 1207.2651
35 X. Liu, Z. G. Luo, and Z. F. Sun, Phys. Rev. Lett., **104**: 122001 (2010)
36 Z. Y. Zhou, Z. Xiao, and H. Q. Zhou, Phys. Rev. Lett., **115**(2): 022001 (2015)
37 S. Uehara et al (Belle), Phys. Rev. Lett., **96**: 082003 (2006)
38 B. Aubert et al (BaBar), Phys. Rev. D, **81**: 092003 (2010)
39 M. Ablikim et al (BESIII), Phys. Rev. Lett., **110**: 252001 (2013)
40 Z. Q. Liu et al (Belle), Phys. Rev. Lett., **110**: 252002 (2013)
41 T. Xiao, S. Dobbs, A. Tomaradze, and K. K. Seth, Phys. Lett. B, **727**: 366 (2013)
42 M. Ablikim et al (BESIII), Phys. Rev. D, **92**(9): 092006 (2015)
43 T. Aaltonen et al (CDF), Phys. Rev. Lett., **102**: 242002 (2009)
44 S. Chatrchyan et al (CMS), Phys. Lett. B, **734**: 261 (2014)
45 V.M. Abazov et al (D0), Phys. Rev. Lett., **115**(23): 232001 (2015)
46 V.M. Abazov et al (D0), Phys. Rev. D, **89**(1): 012004 (2014)
47 X. Liu, S. L. Zhu, Phys. Rev. D, **80**: 017502 (2009); Phys. Rev.D, **85**: 019902 (2012)
48 T. Branz, T. Gutsche, and V. E. Lyubovitskij, Phys. Rev. D, **80**: 054019 (2009)
49 R. M. Albuquerque, M. E. Bracco, M. Nielsen, Phys. Lett. B, **678**: 186 (2009)
50 G. J. Ding, Eur. Phys. J. C, **64**: 297 (2009)
51 F. Stancu, J. Phys. G, **37**: 075017 (2010)
52 Z. G. Wang, Y. F. Tian, Int. J. Mod. Phys. A, **30**: 1550004 (2015)
53 V. V. Anisovich, M. A. Matveev, A. V. Sarantsev, and A. N. Semenova, Int. J. Mod. Phys. A, **30**(32): 1550186 (2015)
54 Z. G. Wang, Eur. Phys. J. C, **63**: 115 (2009)
55 N. Mahajan, Phys. Lett. B, **679**: 228 (2009)
56 R. Aaij et al (LHCb), Phys. Rev. D, **85**: 091103 (2012)
57 J. P. Lees et al (BaBar), Phys. Rev. D, **89**(11): 112004 (2014)
58 T. Aaltonen et al (CDF), Mod. Phys. Lett. A, **32**(26): 1750139 (2017)
59 R. Aaij et al (LHCb), Phys. Rev. D, **95**(1): 012002 (2017)
60 Q. F. L, Y. B. Dong, Phys. Rev. D, **94**(7): 074007 (2016)
61 T. Bhavsar, M. Shah, and P. C. Vinodkumar, Eur. Phys. J. C, **78**(3): 227 (2018)
62 P. Gonzlez, Phys. Rev. D, **92**: 014017 (2015)
63 P. Guo, T. Ypez-Martnez, A. P. Szczepaniak, Phys. Rev. D, **89**(11): 116005 (2014)
64 H. W. Ke, X. Q. Li, and Y. L. Shi, Phys. Rev. D, **87**(5): 054022 (2013)
65 D. Ebert, R. Faustov, and V. Galkin, Mod. Phys. Lett. A, **17**: 803 (2002)
66 N. Brambilla, eConf, **C0610161**: 004 (2006), hep-ph/0702105
67 F. De Fazio, Phys. Rev. D, **79**: 054015 (2009); Phys. Rev.D, **83**: 099901 (2011)
68 G. C. Donald, C. Davies et al, Phys. Rev. D, **86**: 094501 (2012), 1208.2855
69 L. Liu, G. Moir, Peardon et al (Hadron Spectrum), JHEP, **07**: 126 (2012)
70 S. L. Zhu, Y. B. Dai, Phys. Rev. D, **59**: 114015 (1999)
71 V. A. Beilin, A. V. Radyushkin, Nucl. Phys.B, **260**: 61 (1985)
72 S. Godfrey, N. Isgur, Phys. Rev. D, **32**: 189 (1985)
73 T. Barnes, S. Godfrey, and E. S. Swanson, Phys. Rev. D, **72**: 054026 (2005)
74 B. Q. Li, C. Meng, and K. T. Chao (2012), 1201.4155
75 B. Q. Li, K. T. Chao, Phys. Rev. D, **79**: 094004 (2009)
76 L. Cao, Y. C. Yang, and H. Chen, Few Body Syst., **53**: 327 (2012)
77 J. Segovia, A. M. Yasser, D. R. Entem, and F. Fernandez, Phys. Rev. D, **78**: 114033 (2008)
78 E. Eichten et al, Phys. Rev. D, **17**(11): 3090 (1978)
79 W. J. Deng, H. Liu, L. C. Gui, X. H. Zhong, Phys. Rev. D, **95**(3): 034026 (2017)
80 S. Godfrey, K. Moats, Phys. Rev. D, **92**(5): 054034 (2015)
81 Y. Koma, M. Koma, H. Wittig, Phys. Rev. Lett, **97**: 122003 (2006)
82 N. Devlani, V. Kher, and A. K. Rai, Eur. Phys. J. A, **50**(10): 154 (2014)
83 V. Kher, N. Devlani, and A. K. Rai, Chinese Physics C, **41**(7): 073101 (2017), 1704.00439
84 V. Kher, N. Devlani, A.K. Rai, Chinese Physics C, **Vol. 41,**(No. 9), 093101 (2017)
85 N. Brambilla, A. Pineda, J. Soto, and A. Vairo, Rev. Mod. Phys., **77**: 1423 (2005)
86 N. Brambilla et al, Eur. Phys. J. C, **74**(10): 2981 (2014)
87 S. N. Gupta, J. M. Johnson, Phys. Rev. D, **51**(1): 168 (1995)
88 D. S. Hwang, C. Kim, W. Namgung, Phys. Lett. B, **406**: 117 (1997), hep-ph/9608392
89 A. K. Rai, B. Patel, and P. C. Vinodkumar, Phys. Rev. C, **78**(5): 055202 (2008)
90 A. K. Rai, R. H. Parmar, and P. C. Vinodkumar, J. Phys. G: Nucl. Part. Phys., **28**(8): 2275 (2002)
91 E. Eichten, S. Godfrey, H. Mahlke, and J. L. Rosner, Rev. Mod. Phys., **80**: 1161 (2008)
92 M. B. Voloshin, Prog. Part. Nucl. Phys., **61**: 455 (2008)
93 O. Lakhina, E. S. Swanson, Phys. Rev. D, **74**: 014012 (2006)
94 R. Van Royen, V. Weisskopf, Nuovo Cim. A, **50**: 617 (1967)
95 E. Braaten, S. Fleming, Phys. Rev. D, **52**(1): 181 (1995)
96 D. S. Hwang, G. H. Kim, Phys. Rev. D, **55**(11): 6944 (1997)
97 G. J. Ding, J. J. Zhu, and M. L. Yan, Phys. Rev. D, **77**: 014033 (2008)
98 Q. F. Lu, T. T. Pan, Y. Y. Wang, E. Wang, and D. M. Li, Phys. Rev. D, **94**(7): 074012 (2016)
99 F. K. Guo, C. Hanhart, G. Li, U. G. Meissner, and Q. Zhao, Phys. Rev. D, **82**: 034025 (2010)
100 S. F. Radford, W. W. Repko, M. J. Saelim, Phys. Rev. D, **80**(3): 034012 (2009)
101 J. Segovia, P. G. Ortega, D. R. Entem, and F. Fernndez, Phys. Rev. D, **93**(7): 074027 (2016)
102 W. Kwong, P. B. Mackenzie, R. Rosenfeld, and J. L. Rosner, Phys. Rev. D, **37**: 3210 (1988)
103 W. Kwong, J. L. Rosner, Phys. Rev. D, **38**: 279 (1988)
104 A. Bradley, A. Khare, Z. Phys. C, **8**: 131 (1981)
105 G. Belanger, P. Moxhay, Phys. Lett. B, **199**: 575 (1987)
106 Bhaghyesh, K.B. Vijaya Kumar, and A. P. Monteiro, J. Phys. G, **38**: 085001 (2011)
107 H. Negash, S. Bhatnagar, Int. J. Mod. Phys. E, **25**(08): 1650059 (2016)

108 J. H. Yang, S. K. Lee, E. J. Kim, and J. B. Choi (2015), 1506.04481
109 D. Ebert, R. Faustov, V. Galkin, Eur. Phys. J. C, **71**: 1825 (2011)
110 S. F. Radford, W. W. Repko, Phys. Rev. D, **75**: 074031 (2007)
111 D. Ebert, R. N. Faustov, and V. O. Galkin, Phys. Rev. D, **67**: 014027 (2003)
112 M. A. Sultan, N. Akbar, B. Masud, F. Akram, Phys. Rev. D, **90**(5): 054001 (2014)
113 S. Godfrey, N. Isgur, Phys. Rev. D, **32**: 189 (1985)
114 D. Ebert, R. Faustov, and V. Galkin, Eur. Phys. J. C, **66**: 197 (2010)
115 A. Parmar, B. Patel, and P. Vinodkumar, Nucl. Phys. A, **848**: 299 (2010)
116 N. Brambilla et al (Quarkonium Working Group) (2004), hep-ph/0412158
117 E. J. Eichten, K. Lane, and C. Quigg, Phys. Rev. Lett., **89**: 162002 (2002), hep-ph/0206018
118 P. P. D'Souza, M. Bhat, A. P. Monteiro, and K. B. Vijaya Kumar (2017)
119 Bhaghyesh, K. B. Vijaya Kumar, and Y. L. Ma, Int. J. Mod. Phys. A, **27**: 1250011 (2012)
120 F. Giannuzzi, Phys. Rev. D, **78**: 117501 (2008)
121 J. T. Laverty, S. F. Radford, and W. W. Repko (2009), 0901.3917
122 C. R. Munz, Nucl. Phys. A, **609**: 364 (1996)
123 C. S. Kim, T. Lee, and G. L. Wang, Phys. Lett. B, **606**: 323 (2005)
124 D. Ebert, R. N. Faustov, V. O. Galkin, Mod. Phys. Lett. A, **18**: 601 (2003)
125 N. A. Tornqvist, Phys. Lett. B, **590**: 209 (2004)
126 E. Braaten, M. Lu, Phys. Rev. D, **76**: 094028 (2007)
127 M. Albaladejo, F. K. Guo, C. Hanhart, U. G. Meiner, J. Nieves, A. Nogga, and Z. Yang, Chin. Phys. C, **41**(12): 121001 (2017)
128 C. Hanhart, Yu. S. Kalashnikova, A. E. Kudryavtsev, and A. V. Nefediev, Phys. Rev. D, **76**: 034007 (2007)
129 L. Maiani, F. Piccinini, A. D. Polosa, and V. Riquer, Phys. Rev. D, **71**: 014028 (2005), hep-ph/0412098
130 M. Nielsen, S. J. Brodsky (2018), 1802.09652
131 C. W. Zhao, G. Li, X. H. Liu, and F. L. Shao, Eur. Phys. J. C, **73**: 2482 (2013)
132 X. Liu, Z. G. Luo, and Z. F. Sun, Phys. Rev. Lett., **104**: 122001 (2010)
133 F. K. Guo, C. Hanhart, G. Li, U. G. Meissner, and Q. Zhao, Phys. Rev. D, **83**: 034013 (2011)
134 G. Li, Q. Zhao, Phys. Lett. B, **670**: 55 (2008)
135 G. Li, Q. Zhao, Phys. Rev. D, **84**: 074005 (2011)
136 S. S. Afonin, I. V. Pusenkov, EPJ Web Conf., **125**: 04006 (2016)